On the Arrangement of the Micro-crystals in Silver deposited by Electrolysis

AUTHOR(S):

Hirata, Hideki; Komatsubara, Hisaji

On the Arrangement of the Micro-crystals in Silver deposited by Electrolysis.

By

Hideki Hirata and Hisaji Komatsubara.

(Received March 16, 1926)

ABSTRACT

The arrangement of the micro-crystals in silver deposited electrolytically was examined with X-rays. The X-ray-patterns were seen to be explainable with the consideration that the micro-crystals have a tendency to deposit in a fibrous form, and that the diagonal axes of the cubic crystals of silver are arranged parallel to each other as the axis of the fibrous form.

Introduction.

Ever since the ibeas of Laue and Braggs have successfully been realized by experiments, a wide field of investigation bas been opened up in connection with the diffraction phenomena of X-rays by crystals. As one of the extensions of these ideas, the arrangement of the micro-crystals existing in substances has become a subject of the keenest researches. From these researches, it has become evident that the arrangement of the micro-crystals in metals depends largely upon the history of the specimen. Thus, it seems to be of fundamental importance to examine the specimen prepared after some process of a simple and clear nature such as electrolysis, as was the case with Glocker and Kaupp[1] and with Bozorth[2].

So, the writers were also induced, at the kind suggestion of Prof. Masumi Chikashige, to repeat the experiments on the same line with electrolytically deposited silver. Their results are briefly described in the following pages.

1 Z. S. f. Phys., **24**, 121 (1924).

2 Phys. Rev., **26**, 390(1925).

Specimen.

The specimens used were silver electrolytically deposited on a rolled silver plate. Their macro-structures as shown in Plate V, are mossy (Fig. 3, and Fig. 4) or acicular (Fig. 5) according to the conditions of the electrolysis. For the sake of abbreviation, let us call the mossy one specimen A, and the acicular, specimen B, respectively. In the same plate, the micro-structure of these two kinds of specimen are reproduced (Fig. 6, and 7). The conditions under which they were prepared are given below:—

Specimen A:

Electrolyte: 5.5% Ag and 1% free nitric acid.

Potential difference: 1.5 volt.

Current density: 0.02 Amp/cm^2.

Anode: Iron plate thinly covered with Japanese lacquer.

Nineteen vats, each of 60 cms. cube, were arranged in 2 lines; the electrolyte 5.2 cms. deep was flowing from one vat to another at the rate of 6.6 liters per minute. The crystals came to appear after 3 days equally in all the vats.

Specimen B:

Electrolyte (some quantity of silver nitrate being added to the residual liquid in the first experiment): 7.5% Ag. and 0.75% free nitric acid.

Potential difference: 1.5 volt.

Current density: 0.02 Amp./cm^2.

One vat only was used without any flow of the liquid.

Experimental Part.

Outline of the Experimental Method: —In the present experiment, the writers adopted the ordinary "transmission method" founded by Keene[1], Nishikawa[2], and others.

The X-rays emitted from the molybdenum anticathode of a U-type Coolidge tube were cut down by two parallel lead diaphragms. Each of these diaphragms has a circular hole and a narrow pencil of X-rays passing through these holes was made to strike the specimen to be tested. The photographic plate was placed perpendicularly to the incident beam in a position a few cms. behind the specimen.

To excite the tube, a transformer was employed. The maximum voltage measured by the length of a spark gap between needle-points was

1 Phil. Mag., **26**, 712 (1913).

2 Proc. Tokyo Math. Phys. Soc., **7**, 131 (1913).

about 50–70 K. Vs., and the current through the tube was 4–5 milliamperes. The time of exposure varied from 27 to 32 hours according to the condition.

Discussion of the Experimental Result:

(i) Specimen A: Some finest fragments, of this specimen with which the experiment was first performed, had been pasted on a sheet of paper, so that the face of each lamella was parallel to the surface of the paper. When the common face of these lamellae, which coincided with the surface of the paper, was set perpendicular to the incident beam, then the interference figure reproduced in Fig. 8, Plate VI was obtained on the photographic plate placed 3.2 cms. behind the specimen.

In this figure, the prominent part of the blackening consists of a number of concentric circular rings, and the central spot impressed by the undeflected beam.

It is evident that the interference figure under consideration is essentially the same as those obtained by Debye-Scherre, and Hull by the powder method: the concentric rings are considered to be produced when the arrangement of the micro-crystals in the specimen has no regularity with regard to the direction of the incident beam.

If we inspect Fig. 8 more minutely, it will be observed that this figure consists of a large number of bands radiating outward from the central spot, and that, the concentric rings in the figure are nothing but an assemblage of a large number of intense spots on the radiating bands. This point seems to be a little different from the figure obtained by the ordinary powder method, and the reason will be given later on.

Fig. 12 and Fig. 9 are the interference figures taken in a similar way as Fig. 8 with a larger fragment of specimen A. To obtain these two figures, a piece of the mossy crystal of moderate size (0·8–1·2 mms. in dia.), and a very large piece which was rather foliate (about 4 mms. in width) were used, respectively. As in the previous case, the photographic plate was placed 3·2 cms. behind the specimen in both cases.

The prominent parts of these two figures, Fig. 12 and Fig. 9 consist of several bands radiating outward from the central spots. In the former figure, there are 6 prominent linear bands, any one of them making an angle of about 60° with the neighbouring bands on either side; while the latter figure consists of 24 prominent wide radiating bands of rather triangular shapes. On the whole, they present the symmetrical interference figures, and each of them has a unmber of intense spots on it, which seem to be registered by the characteristic radiations

from the target.

It will easily be noticed by putting Fig. 12 upon Fig. 9 that 6 prominent bands in Fig. 12 coincide with the central lines of the most intense triangular shaped bands in Fig. 9 which are denoted by I' in the figure. Moreover, by reducing the diameters of the slits to about 0·8 mms., the same interference figures as Fig. 12 were also obtained, even when a piece of the large foliate crystal was used. These facts show that there must exist some connections between the arrangements of the micro-crystals of the two samples to give rise to the two different figures under consideration.

It can also be noticed that the distance from the central spot to any one of the intense spots in Fig. 12 and Fig. 9 is equal to the radius of one of the concentric rings represented in Fig. 8, Plate VI. This equality of distances suggests the existence of some relations between these figures.

The annexed Fig. 1, represents diagrammatically the central lines of the radiating bands in Fig. 9 as well as the positions of the intense spots on the bands. In this figure, the intensity of each band is shown by the thickness of the corresponding line. As the first approximation,

Fig 1. The Standard Figure.

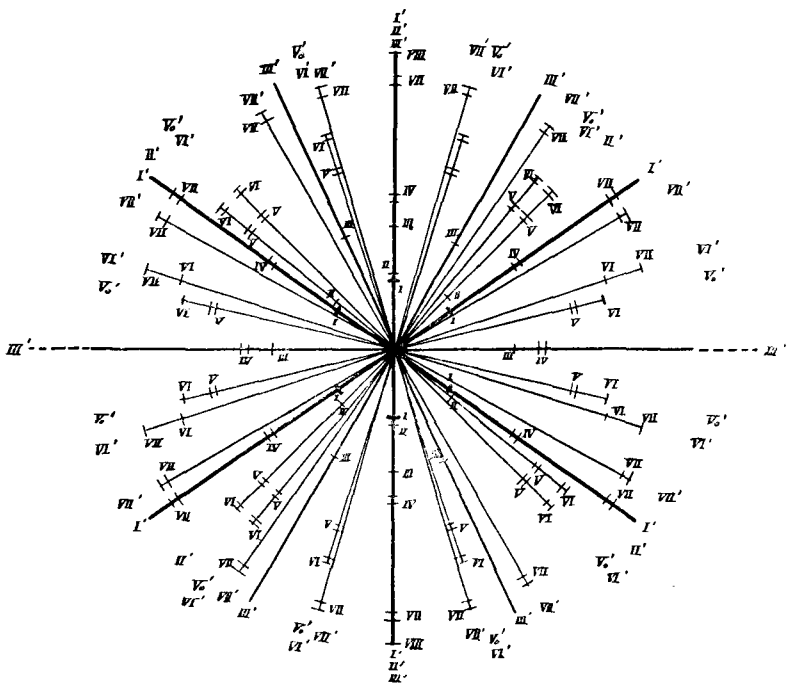

the lines representing the position of the central lines of the triangular bands were drawn as straight lines because the curvature was insignificant.

Now suppose that there is an arrangement of micro-crystals which will induce the interference figure characterized by the condition, that all the radiating bands in this figure are nearly linear, and that the distribution of the radiating bands are those given in Fig. 1. For the sake of convenience, we shall call all the figures, the same as that represented in Fig. 1, the "standrad figures."

In the standard figures, it will be noticed that the intense spots represented by I' coincide with the radiating bands reproduced in Fig. 12, Plate VII. Moreover, the same figures as Fig. 8, and Fig. 9, in Plate VI, can be obtained by overlapping many of these standard figures: To get the same figure as Fig. 9, the many standard figures should be placed one upon another in such a way that the central spot of each figure coincides with the others, and that all the correspoding radiating bands in the figures are displaced a little, within about 5°. The same figure as Fig. 8 can be realized, when these standard figures are irregularly overlapped by keeping their central spots on the same point.

From the above consideration, it may be quite possible to suppose that the arrangement of the micro-crystals to produce the standard figure and those to produce Fig. 8, Fig. 9, and Fig 12, are essentially the same.

At this stage it may be well to note the condition under which such a standard figuer is produced. As is already known, the radiating bands are produced only when the specimen is fibrous; i. e., the micro-crystals in the specimen are mostly so arranged that a certain definite axis of every crystal is arranged in the same direction, but that in other respects the orientation is at random.

As a result of many researches with such fibrous specimens, the following facts are also well known:

(a) If the axis of the fibrous arrangement is placed perpendicularly to the direction of the incident beam, the figure consists of a set of nearly straight bands passing through the central spot; (b) If, however, the axis is inclined against the plane normal to the incident ray, the figure is altered; the radiating bands in this figure are not nearly straight but are γ shaped; (c) In the extreme case, when the axis of the fibre is brought parallel to the incident ray,the figure obtained is a set of concentric rings around the central spot.

Thus considered, it will easily be seen that the orientation (a) of the fibrous arrangement applies well to the case which will give rise to the standard figure.

The intense bands in the standard figure, as already stated, coincides well with Fig. 12, Plate VII. It would seem, accordingly, to be presumable that the latter figure would also be obtained by the orientation (a),

Thus, it seems to be quite legitimate to accept the following two statement:—

(1) The micro-crystals in the moderate sized lamella are mostly so arranged that they have a definite common axis, and any reflection plane is inclined with a definite angle to the direction of this axis, but that in other respects the orientation of the reflecting plane is irregular.

(2) The direction of the common axis is perpendicular to the direction of the incident ray. Therefore, the common axis should be situated on the face of the lamella.

As was stated before, the photograph, Fig. 8 was obtained with a specimen consisting of a large number of fine lamellae. If we assume that each lamella in this case contains micro-crystals of the same fibrous arrangement as that in a moderate sized lamella, then Fig. 8 is capable of immediate explanation.

Now, before entering into details, let us determine the indices of each atomic plane, by the reflection of which the concentric rings are formed.

From the researches of Vegard[1], Kahler[2], Gerlach[3], it is known that the crystal of silver is of a face-centred cubic lattice, the one side of the elementary cube being 4.06 A. U, long. From these data, the spacing of each atomic plane can be calculated.

In Table 1, the indices of the prominent atomic planes, and the calculated values of the corresponding spacings d are represented.

Table. 1.
The Calculated Values of d.

Indices of Planes	d in 10^{-8} cm.
(111)	2·34
(100)	2·03
(110)	1·44
(210)	0·91
(211)	0·83

The numerical values of d can also be caluclated from the radii of the concentric rings in Fig. 8. If we denote the value of a spacing by d, the wave length of the characteristic radiation giving rise to a ring by λ, the distance of the photographic plate from the sample by L and the radius of a ring by r, then we have the following weell known relations between them.

$$2\,d \sin\theta = n\lambda \quad \ldots\ldots(1)$$

$$L \tan 2\theta = r \quad \ldots\ldots(2)$$

1 Phil. Mag., **31**, 83 (1916).
2 Phys. Rev., **8**, 210 (1921).
3 Z. S. f. Phys., **9**, 184 (1922).

where n is a positive integer representing the order of the spectrum, and $\theta = \frac{\pi}{2} - \gamma$ is the glancing angle.

Now for the sake of convenience, let us denominate the concentric rings by I, II, III, IV, V, VI, VII and VIII respectively in order of increasing radius. By measuring the radii of these rings, we obtain the numerical values of r as shown in the second column of Table 2. If we substitute these numerical values of r, and L = 3.2 in equation (2) successively, the value of θ corresponding to each ring will be obtained. The values of θ thus calculated are given in the third column of Table 2. With these values of θ the values of $\frac{d}{2}$ which are given in the fourth column of Table 2, will be found from equation (1) by assigning to λ the value of the wave length of the Kα line of molybdenum. Though it may be possible that the Kβ line of molybdenum will also appear, but as the intensity of this line is very feeble compared with that of the Kα line, we have taken

Table. 2.

No. of Rings	r in cm.	θ	$\frac{d}{n}$ in cm.	n	d in 10^{-8} cm.	Calculated Values: d in 10^{-8} cm.	Calculated Values: Indices of Planes	Indices of the Reflecting Planes
I	1·01	8°46′	$2{\cdot}33^{9}$	1	2·34	2·34	(111)	$(111)_{I}$
II	1·17	10° 3′	$2{\cdot}03^{3}$	1	2·03	2·03	(100)	$(100)_{I}$
III	1·79	14°37′	$1{\cdot}40^{6}$	1	1·41	1·44	(110)	$(110)_{I}$
IV	2·26	17°37′	$1{\cdot}17^{5}$	2	2·35	2·34	(111)	$(111)_{II}$
V	2·77	20°26′	$1{\cdot}01^{6}$	2	2·03	2·03	(100)	$(100)_{II}$
VI	3·29	22°54′	$0{\cdot}91^{2}$	1	0·91	0·91	(210)	$(210)_{I}$
VII	4·03	25°47′	$0{\cdot}81^{6}$	1	0·82	0·83	(211)	$(211)_{I}$
VIII	4·44	27° 7′	$0{\cdot}77^{9}$	3	2·34	2·34	(111)	$(111)_{III}$

the Kα line only. For the value of the wave length of the Kα line, we have given the mean value of the $K\alpha_1$ and $K\alpha_2$ lines, which is equal to $\lambda\alpha = 709.73 \times 10^{-11}$ cm.

Each one of the unmerical values of $\frac{d}{n}$ in the fourth column of Table 2, should represent a spacing or its submultiple of the silver crystal. Consequently, by assigning an adequate positive integer to n, the numerical value of d will be obtained from each one of the values of $\frac{d}{n}$.

Now assigning to n the integers as shown in the fifth column of Table 2, the numerical values of d in the sixth column are obtained. As was to be expected, each one of these numerical values agrees well with one of the calculated values in Table 1, which are here rewritten in the seventh column of Table 2. The indices of the atomic planes corresponding

to the spacings given in the seventh column — and consequently in the sixth column — of Table 2 are tabulated in the eighth column. Thus it seems to be legitimate to assign the indices of the atomic planes and the order of the spectra as given in the ninth column to each concentric ring. The symbols ( )I, ( )II, and ( )III in the ninth column denote the order of the spectrum.

Next, let us determine separately the indices of the atomic planes which are responsible for causing the radiating bands. This determination was attempted in the same way as performed by S. Tanaka[1], and T. Fujiwara[2] who made use of the position of the intense spots on each radiating band.

In Table 3, the first column represents the numbers of the radiating bands marked in Fig. 9, Plate VI, or in Fig. 1. The numbers of the intense spots on each radiating band are given in the second column. Here it must be noted that the intense spot is denoted by the same numbes as that of the correspondind concentric ring.

Table. 3.

No. of Radiating Bands	No. of Intense Spots	Indices of the Planes
III′	III, IV,	$(1,1,0)_{I}$
V$_0$′	V, VI,	$(3,3,1)_{I}$
VI′	VI, VIII,	$(2,1,0)_{I}$
VII′	VII,	$(2,1,1)_{I}$
I′	I, IV, VII,	$(1,1,1)_{I\ II}$
II′	II, V, VI,	$(1,1,0)_{I}$
V$_0$′ VI′	V, VI,	$\begin{cases}(2,1,0)_{I}\\(3,3,1)_{I}\end{cases}$
VII′	VII,	$(2,1,1)_{I}$
III′	III,	$(1,1,0)_{I}$
V^{o} VI′	V, VI,	$\begin{cases}(2,1,0)_{I}\\(3,3,1)_{I}\end{cases}$
VII′	VII,	$(2,1,1)_{I}$
I′ II′ III′	I, II, III, IV, VII, VIII	$\begin{cases}(1,0,0)_{I\ II}\\(1,1,0)_{I\ II}\\(1,1,1)_{I\ II\ III}\end{cases}$

The orders of the spectrum and the indices of the atomic planes belonging to these spots should be the same as those of the corresponding concentric rings, These were already given in Table 2, and they are tabulated again in the third column of Table 3. It is clear that the atomic plane which gives rise to the intense spots on a radiating band should also give rise to this radiating band. Consequently, we can regard the indices of the atomic planes given in the third column of Table 3 as those giving rise to the bands represented in the first column of the same table.

From the angular distribution of the radiating bands the axis of the micro-crystals arranged in the direction of the axis of the fibre will be determined. For this purpose a calculation was carried out as was done

1 These Memoirs, **8**, 319 (1925).
2 These Memoirs, **8**, 339 (1925).

by A. Ono,[1] who made use of the following relation.

$$\cos\beta = \cos\gamma\cos\alpha + \sin\gamma\sin\alpha\cos\varphi \quad \ldots\ldots\ldots\ldots(3)$$

where α is the angle between the incident ray and the fibrous axis of the crystals, β the angle between the normal of a certain reflecting plane and the fibrous axis of the crystals, γ the angle between the incident ray and the normal of the reflecting plane, and φ the azimuth of a point on a radiating band measured on the photographic plate, from the direction parallel to the fibrous axis of the crystals by taking the central spot as the pole.

From the above relation (3) and equation (2), each radiating band will be traced out, for a definite value of α and β, by giving various values to γ, and the by finding the numerical relations between φ and r. It will easily be seen that, when $\alpha = \frac{\pi}{2}$ at the vicinity of the central spot, the radiating bands will become nearly straight, and that the value of φ will be nearly equal to β. Thus, if the value of β is found by measuring the angles between the bands, the axis of the crystals arranged in the direction of the axis of the fibre will be known immediately.

Generally, taking a corner atom of the cubic lattice as the origin of a rectangular co-ordinate system and the edges of the cubic lattice as the axis of the co-ordinates, the angle β corresponding to an atomic plane with the indices h_1, h_2, h_3 will be given as follows:—

$$\cos\beta = \frac{h_1 l' + h_2 m' + h_3 n'}{\sqrt{h_1^2 + h_2^2 + h_3^2}} \quad \ldots\ldots\ldots\ldots(4)$$

where l', m', n': the direction cosines of the common axis of the crystals.

Now let us provisionally assume that the axis of the fibrous arrangement of the specimen coincides with a diagonal axis of the cubic lattice. Then the values of l', m' and n' will become

$$l' = 0 \qquad m' = n' = \frac{1}{\sqrt{2}} \quad \ldots\ldots\ldots\ldots(5)$$

and the expression (4) is reduced to

$$\cos\beta = \frac{h_2 + h_3}{\sqrt{2}\sqrt{h_1^2 + h_2^2 + h_3^2}} \quad \ldots\ldots\ldots\ldots(6)$$

From this equation, by assingning proper values to h_1, h_2, h_3 we obtain the values of β belonging to each atomic plane. The values thus obtained, are given in the left side of the Table 4.

On the other hand, the results of observations are given in the right side of Table 4, The values of β here given are obtained from Fig. 1,

1 Mem. Coll. Engineering, Kyushu, **2**, 247 (1922).

Table. 4.

Calculated Values		Observed Values		
Indices of Pls. h_1, h_2, h_3	β	No. of Rad. Bds.	β	Indices of the Families of Pls.
1, 1, 0	0°	III′	0°	(1, 1, 0)
3, 3, 1	13°13′	V$_0$′	13°	(3, 3, 1)
0, 2, 1	18°23′	VI′	18°	(2, 1, 0)
1, 2, 1	30° 1′	VII′	30°	(2, 1, 1)
1, 1, 1 $\bar{1}$, 1, 1	35°16′	I′	35°	(1, 1, 1)
0, 0, 1	45°	II′	45°	(1, 0, 0)
3, 3, 1	49°32′	V$_0$′ VI′	50°	(2, 1, 0) (3, 3, 1)
1, 2, 0	50°56′			
2, 1, 1	54°45′	VII′	54°	(2, 1, 1)
1, 1, 0 1, $\bar{1}$, 0	60°	III′	60°	(1, 1, 0)
3, 3, $\bar{1}$	71° 4′	V$_0$′ VI′	71°	(2, 1, 0) (3, 3, 1)
2, 1, 0	71°34′			
1, 2, 1	73°14′	VII′	73°	(2, 1, 1)
1, 0, 0	90°	I′ II′ III′	90°	(1, 0, 0)
0, $\bar{1}$, 1				(1, 1, 0)
1, 1, 1				(1, 1, $\bar{1}$)

by measuring the inclination of each radiating band, and the indices of the atomic plane corresponding to it are taken from Table 3, which have previously been obtained from the position of the intense spots. As for the direction parallel to the axis of the fibrous arrangement in Fig. 1, from which the inclination of each radiating band is measured, we took the horizontal bands III′ produced by the atomic plane (1, 1, 0).

Comparing the calculated and the observed values in Table 4. we observe that the agreement is fairly well within the limit of experimental errors. Next the writers tried to ascertain whether this result be also explainable by taking the prominent axes other than the diagonal of the crystal as the axis of the fibrous arrangement, but it was a failure. Accordingly it will not be unnatural to conclude that in the case of the standard figure the axis of the micro-crystals in the sample are arranged in a fibrous arrangement, and that the diagonal axes of the crystals are arranged in the direction of the axis of the fibre, which is parallel to the surface of the lamella.

As the consequence of our foregoing argument in connection with Fig. 8, Plate VI and Fig. 12, Plate VII, we may apply well the preceding

conclusion to the case when the fragment is not so large as in the case of Fig. 9, Plate VI. In such cases too, the arrangement of the micro-crystals in one of the mossy pieces will be the same as that of the standard figure. Fig. 9, obtained with a large foliated piece may easily be understood, if we consider that the foliated piece consists of many small lamellae of fibrous arrangement the axis of the fibre being distributed within the angular extension of each strip in the plane parallel to the surface of the lamella.

In short the arrangement of the micro-crystals in the specimen A may be summarized in the following two statements.

(1) Every piece of Specimen A consists of one lamella or several lamellae of fibrous arrangement, taking the diagonal axis of each cubic lattice as the axis of the fibre.

(2) When there exist a number of lamellae of fibrous arrangement in one piece of the specimen, the direction of the fibres are not strictly the same.

Next, to confirm the above consideration, the writers investigated the interference phenomena obtained in two orientations of the samples, one when it was rotated 22° around the direction parallel to the axis of the fibre, and the other when it was rotated 22° around an axis perpendicular to the axis of the fibre.

In both cases, the interference figures were photographed with the same large foliated fragment as was used in the case of Fig. 9, Plate VI. The distance between the photographic plate and the specimen was 3.5 cms. If our consideration be correct, the figure in the former case should remain unaltered; while in the latter case the symmetry of the figure should be violated. As was expected, the same interference figure Fig. 9, Plate VI, was obtained in the former case, but in the latter case the interference figure was quite different from the former one. Fig. 11, Plate VI is the photograph taken when the axis of the fibre was tilted from its vertical position toward the incident ray.

It is presumable that the same radiating bands as in Fig. 11 may be traced, if we find the relations between φ and θ, and between θ and r for a definite value of β corresponding to each atomic plane. To obtain the values of φ corresponding to values of θ from equation (3), the values of β given in Table 4 were employed, and for the values of α two values of $90^\circ - 22^\circ = 68^\circ$ and $90^\circ + 22^\circ = 112^\circ$ were taken. The values of φ corresponding to $\alpha = 68^\circ$, are given in the upper half of Table 5, and those corresponding to $\alpha = 112^\circ$, are given in the lower half of the same

table. The values of r corresponding to various of θ are calculated from equation (2) and they are given in Table 6. In Fig 2, the upper half corresponds to the case when $\alpha = 68°$, and the lower half corresponds to the case when $\alpha = 112°$.

Table. 5.
The Numerical Values of φ
(The Upper of Fig. 2)

θ \ β	0°	13°13′	18°23′	35°16′	45°	60°	90°
0°	—	—	—	28°17′	40°18′	57°22′	90°
3°	—	—	—	30°36′	42° 3′	58°45′	91°13′
5°	—	—	7°18′	31°57′	43° 6′	59°37′	92° 2′
10°	—	5°46′	14°32′	34°37′	45°18′	60° 5′	94° 5′
15°	—	11°49′	17°57′	36°32′	47° 3′	63°15′	96°13′
20°	—	14°	19°36′	37°48′	48°21′	64°44′	98°27′
30°	—	11°45′	18°29′	38°25′	49°39′	67° 5′	103°29′

(The Lower Half of Fig. 2)

θ \ β	0°	13°13′	18°23′	35°16′	45°	60°	90°
0°	—	—	—	28°17′	40°18′	57°22′	90°
3°	—	—	—	25°10′	38°17′	55°52′	88°47′
5°	—	—	—	23°10′	36°46′	54°47′	87°58′
10°	—	—	—	15° 7′	32°15′	51°46′	85°55
15°	—	—	—	—	26° 8′	48°19′	83°47′
20°	—	—	—	—	16°32′	46°52′	81°33′
30°	—	—	—	—	—	58° 8′	76°31′

The part of the figure represented by the shadow in Fig. 2 is the copy of the figure of Fig. 11, Plate VI, while that represented by the thick full lines is the calculated lines corresponding to $\beta = 35°16'$ and $\beta = 90°$. These lines are caused by the reflection from the most prominent reflection plane (1,1,1), and they correspond to the strongest bands marked by I′ in the case of the normal incidence of the X-rays. As may be seen from the figure, the agreement between the calculated curves and the observed ones is satisfactory.

Table. 6.

θ	r
0°	0
3°	0, 3 7
5°	0, 6 2
10°	1, 2 7
15°	2, 0 2
20°	2, 9 4
30°	6, 0 6

(ii) Specimen B; This specimen can be classified in two parts, i. e., the main acicular part which has many long edges along its axis, and the granular part cosisting of many granules aggregated at the foot of the acicula.

Fig. 2

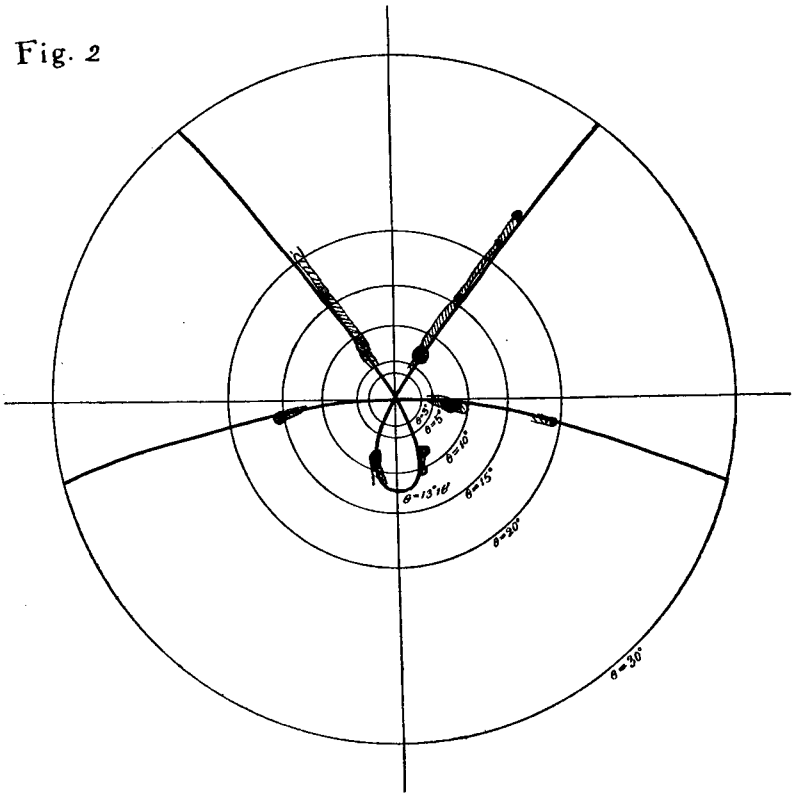

The Main Part:— By placing the axis of the acicular part parallel to the incident ray, we obtained the figure reproduced in Fig. 13, Plate VII. When the same axis was placed perpendicularly to the direction of the incident ray, so that the incident ray might sweep the periphery of the specimen the interference figure as shown in Fig. 14 Plate VII was obtained. In both cases, the photographic plates were set perpendicular to the incident beam in a position 3.2 cms, behind the specimen.

The prominent part of the figure reproduced in Fig.13, Plate VII consists of a set of Debye-Hull's rings associated with several Laue's spots. Though, the presence of Laue's spots shows that there are crystals of considerable dimensions, we may, however, from the predomination of Debye-Hull's rings, conclude that the majority of the micro-crystals in the specimen are irregularly orientated with respect to the direction of the incident ray.

Now, having confirmed that most of the micro-crystals in the specimen are irregularly orientated with respect to the direction of the incident ray,

only the following two cases are conceivable: —

(1) The case when the majority of the micro-crystals are irregularly orientated with respect to any direction.

(2) The case when the micro-crystals in the specimen are mostly so arranged that they have a definite common axis parallel to the acicular axis.

In order to decide which of these is the right one, let us consider the interference figure reproduced in Fig. 14.

In this figure, a set of radiating bands are predominant, which coincide well with the bands assigned by the same marks Ⅰ′ Ⅱ′, Ⅲ′ etc, in Fig. 1. Moreover, the intense spot on each radiating band of Fig. 14, comes out at the same position as that of Fig. 1. We may consequently conclude that the second case before mentioned applies well to the present arrangement. The fact that the interference figure in Fig. 14, Plate VII is essentially the same as the standard figure, indicates that the arrangement of the micro-crystals corresponding to the case of Fig. 14 should be the same as that corresponding to the standard figure, and that the micro-crystals in the acicular part should be mostly so arranged that the diagonal axis of each micro-crystal coincides with the acicular axis.

It can be expected from the above considerations that the acicular direction represented by ←→ in Fig. 14, should coincide with the direction of the axis of the fibrous arrangement, i. e., the direction of the radiating band Ⅲ′ belonging to the atomic plane 1, 1, 0. This expectation is also confirmed.

The consideration hitherto mentiond in connection with the acicular part lead us to the following conclusion:— The micro-crystals in the main acicular part of Specimen B are mostly so arranged, — similar to the case of Specimen A, — that the diagonal axis of each lattice coincides with the direction of the acicular axis, and that in other respects the orientation is at random.

In order to know whether the above conclusion may hold also good even in the inner region of the acicula, the writers experimeted with a specimen which was prepared by pickling the acicular part in dilute nitric acid. When the acicular part was pickled for a moderate time, it was disintegrated into several lamellae whose surfaces were parallel to the acicular direction. By transmiting the incident ray through a lamella placed normally to its direction, we obtained the figure reproduced in Fig. 10, Plate VI. This figure was essentially the same as that shown in Fig. 14, Plate VII.

Consequently, we know that the foregoing conclution in connection with the arrangement of micro-crystals in the periphery of the specimen holds also good even in the inner region of the specimen.

Granular Part: — The micro-structure of this part is shown in Fig. 7, Plate V. A number of twined crystals are vissible in this figure.

With a piece of this specimen, we obtained the figure which was reproduced in Fig. 15, Plate VII the distance between the specimen and the photographic plate being also 3.2 cms. in the present case. The prominent part of this figure consists of the complex mixture of Laus's spots, radiating bands, and Debye-Hull's rings.

From this figure, we may suppose that the most part of a granule consists of the irregular deposition of the micro-crystals, which contains several crystals of considerable size and of the fibrous arrangement. Furthermore, it may be natural to speculate that the fibrous pieces in this disposition are small fragments of the same constitution as those mentioned bofore.

From our foregoing argument in connection with Specimens A and B, we arrive at the following conclusions:—

(1) The silver micro-crystals have a tendency to deposit in the fibrous form.

(2) The diagonal axis of each cubic lattice is arranged in a direction parallel to the axis of the fibre.

The above conclusions contradict those of Glocker[1] and Bozorth[2], who endeavoured to suggest that electrolytically deposited silver has no regular orientation.

In conclusion, the writers wish to express their best thanks to Professor. M. Chikashige for his kind suggestions and interest, and to Professor. U. Yoshida for his kind guidance during the progress of experiment. Our thanks are also due to Mr. T. Miyoshi, by whose kind assistance some of the microscopic investigations were made.

1 Loc. cit.

2 Loc. cit.

Fig. 3. Macro-structure of Specimen A
(view of transversal section)

Size 1 : 1½

Fig. 4. Macro-structure of Specimen A
(view of longitudinal part)

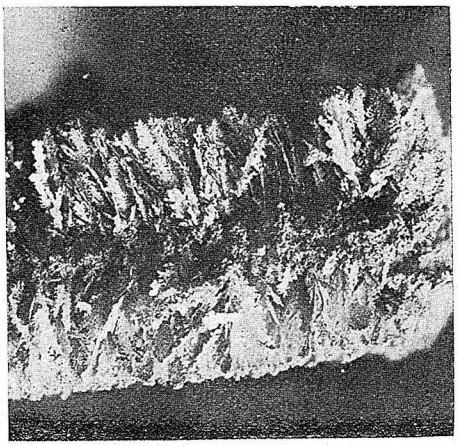

Size 1 : 1½

Fig. 5. Macro-structure of Specimen B
(normal deposit)

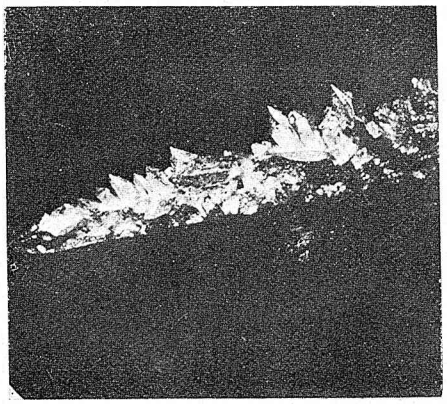

× 18

Fig. 6. Micro-structure of Specimen A
(mossy part)

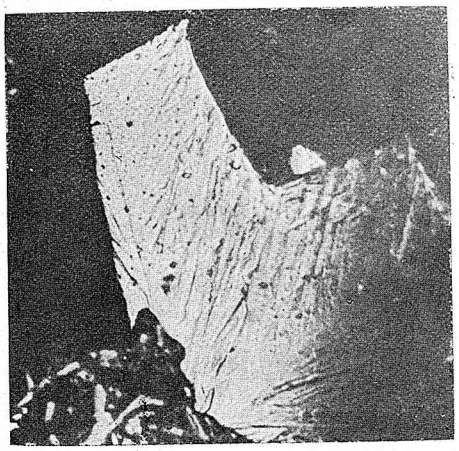

× 200

Fig. 7. Micro-structure of Specimen B
(granular part)

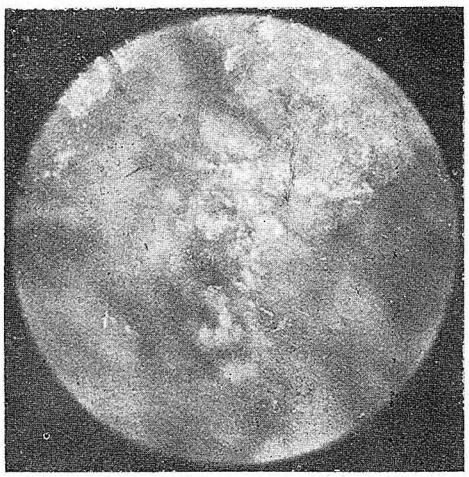

× 140

Fig. 8. Specimen A

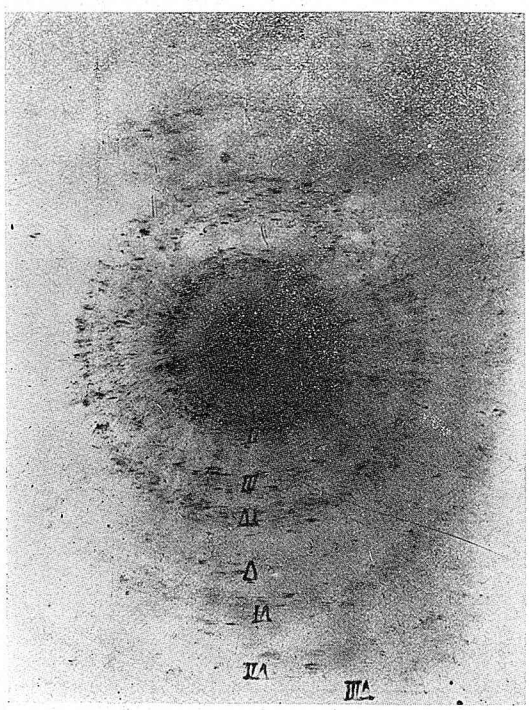

Fig. 9. Specimen A

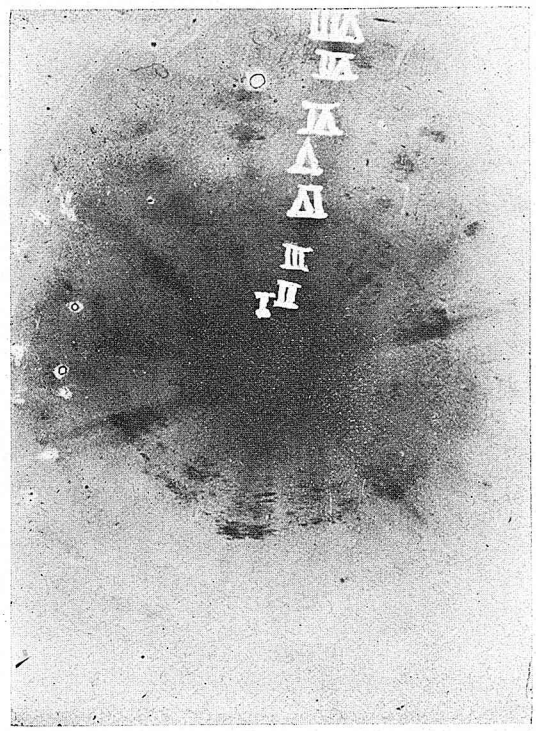

Fig. 10. Specimen B main part (inner)

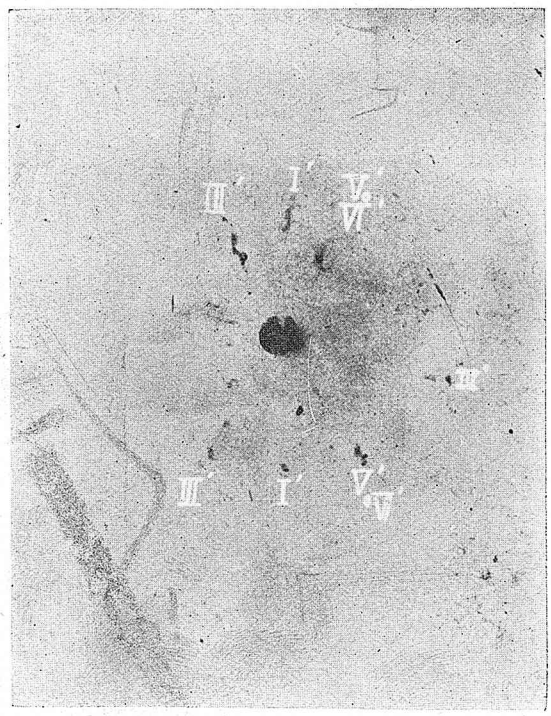

Transversal

Fig. 11. Specimen A

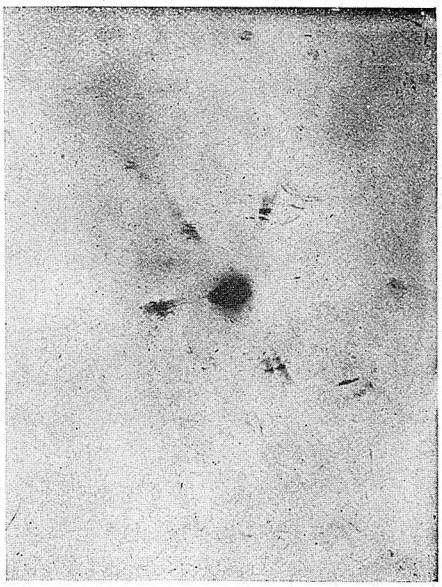

Fig. 12 Specimen A

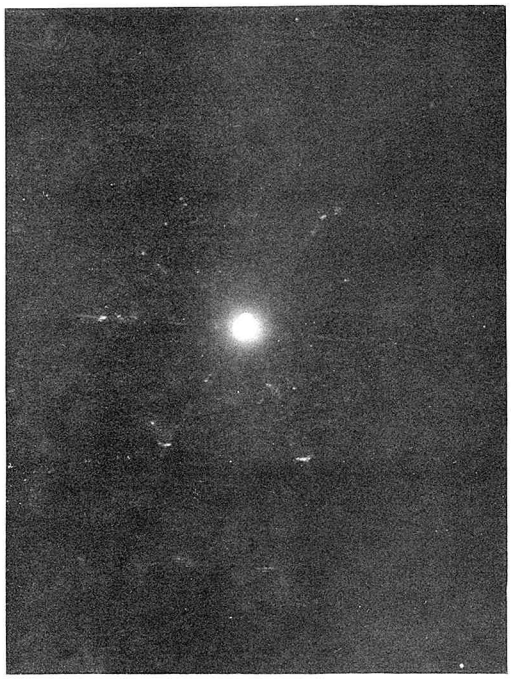

Fig. 13. Specimen B main part

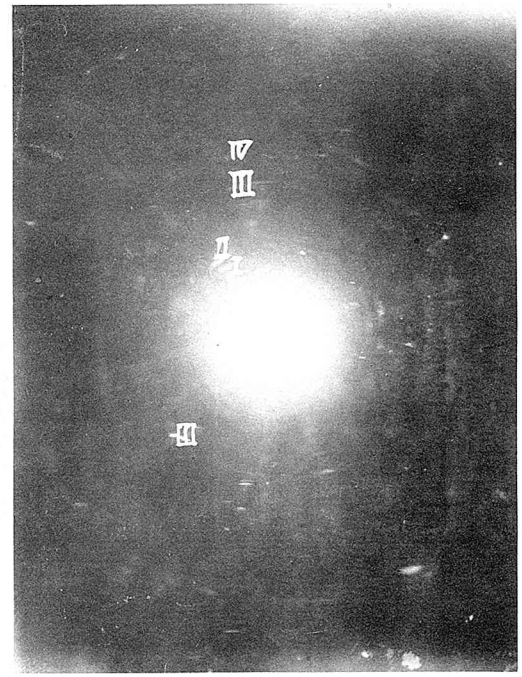

Longitudinal

Fig. 14. Specimen B main part (periphery)

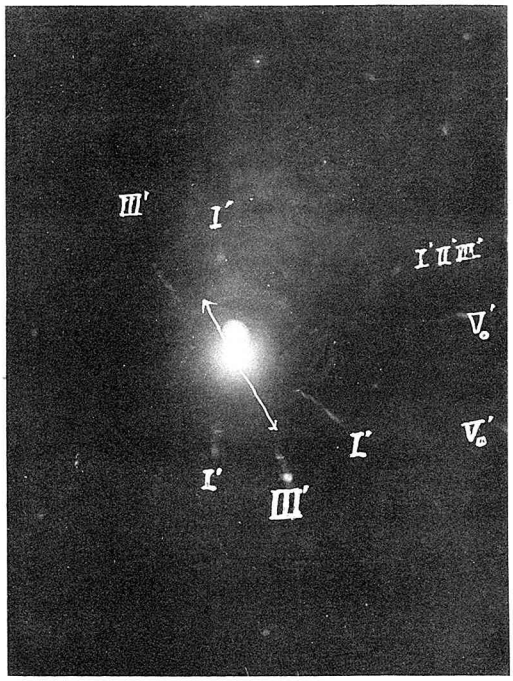

Transversal

Fig. 15. Specimen B granular part